International Journal of the Physical Sciences Vol. 6(12), pp. 2789-2798, 18 June, 2011
Available online at http://www.academicjournals.org/IJPS
DOI: 10.5897/IJPS11.599
ISSN 1992 - 1950 ©2011 Academic Journals

Full Length Research Paper

Improvement of direct torque control in high power induction motors

A. Gandomkar[1]*, A. Mahmoudi[1,2], H. Pirasteh[3], A. Parastar[4] and S. Kahourzade[1]

[1]Faculty of Engineering, University of Malaya, 50603 Kuala Lumpur, Malaysia.
[2]Engineering Department, HELP College of Arts and Technology, Jalan Metro Pudu 2, Fraser Business Park, 55200 Kuala Lumpur. Malaysia.
[3]Electrical Engineering Department, K. N University of Technology, Tehran, Iran.
[4]Department of Electrical Engineering, Yeungnam University, Daegu, South Korea.

Accepted 16 May, 2011

Matrix converter rather than voltage source inverter can be used as high-performance technique supplying electric motor in direct torque control (DTC). DTC's most significant deficiency in induction motor, magnetic torque ripple, can be markedly reduced by appropriate space voltage-vectors whose influence on stator flux and electromagnetic torque in DTC of induction machine that uses "matrix converter" the subject of this work. DTC degrees of freedom were shown seriously limited by 60° flux sectors, thus division to twelve 30° sectors of flux-space vector hexagon is proposed. The increased "matrix converter" degrees of freedom were then extracted for DTC implementation.

Key words: Induction motor, direct torque control, matrix converter.

INTRODUCTION

Direct torque control (DTC) technique for induction motors was first introduced by Takahashi in the mid-1980s, for direct control of electromagnetic torque and motor flux (Takahashi and Noguchi, 1986). It allows both simultaneous and independent control of electromagnetic torque and motor flux. Its main advantages are fast torque response, robustness against parameter variation, absence of PWM pulse generation and current regulators, and no requirement for these: speed/position sensors, coordinated transformation and decoupling processes for voltage and currents (Lascu et al., 2000). Its main drawback, however, is the high current and the torque ripple. Disadvantages also include variable switching frequency, and at very low speeds, difficult-to-control torque and flux (Zaid et al., 2009). Suitable voltage vectors can reduce motor torque ripple effectively. A "matrix converter" enables control of torque and flux through various vector-selection criteria which give rise to various switching strategies, each affecting drive torque ripple, current ripple and switching frequency (Vargas et al., 2010). Ac-ac "matrix converter" is a good alternative to conventional ac-dc-ac converter, for interfacing of two ac systems at various voltages and/or frequencies (Hojabri et al., 2011; Klumpner et al., 2007). Its advantages include sinusoidal input and output waveforms, bidirectional power flow, and fully-controllable input power factor. It needs neither dc-link circuit nor large storage element (for example, capacitor), thus size and volume reduce, and reliability increases through the missing-dc-link's allowance for a compact design. These features earn the topology's industrial application in DTC drive systems. Various works propose various voltage-vector-selecting strategies for DTC drive with "matrix converter" (Casadei et al., 2001; Lee et al., 2007; Lee and Blaabjerg, 2007, 2008; Ortega et al., 2010). The methods presented have various influences (for example, current ripple and torque ripple) on drive system, though exact influences on stator flux and electromagnetic torque for use in accurate selection algorithm have yet to be reported.

This work extracted the basic equations for flux

*Corresponding author. E-mail: gandomkar.ali@gmail.com Tel: +60123572072. Fax: 03-79675317.

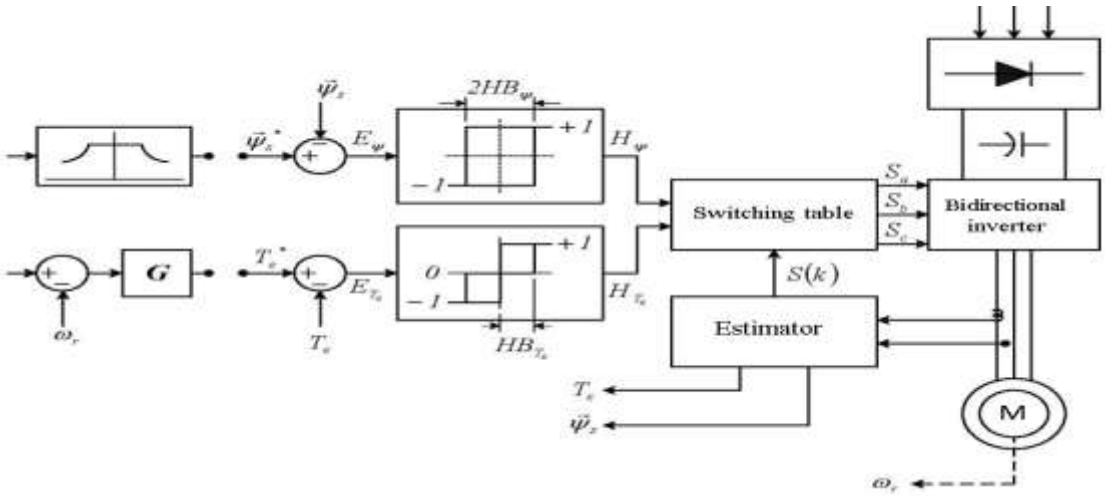

Figure 1. Direct torque control block diagram (Bose, 2002).

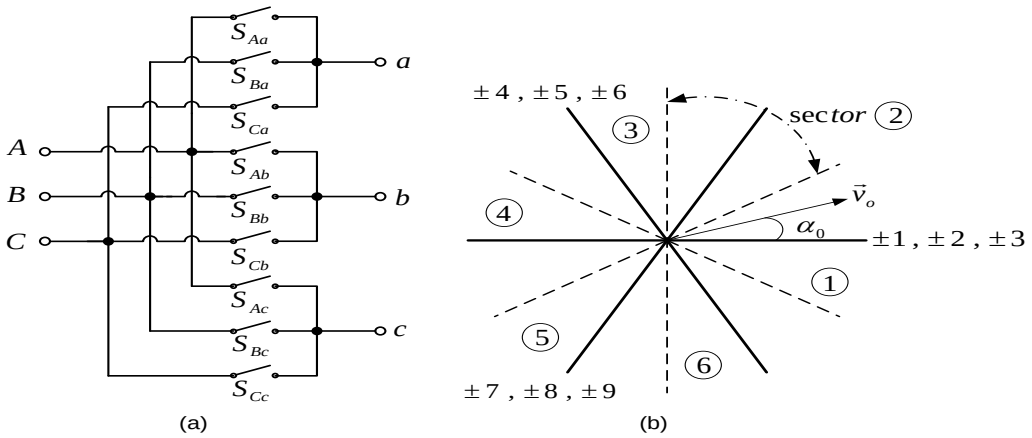

Figure 2. (a) 3 × 3 matrix converter; (b) and active voltage vectors produced by matrix converter.

variation and torque variation; they were then used to investigate the effect of each voltage vector on motor flux and electromagnetic torque. DTC matrix-converter degrees of freedom were then extracted, and an appropriate switching table proposed. The following study introduces the fundamentals of "matrix converter" and principles of DTC, then explore basic equations for flux and torque variations.

Fundamentals of direct torque control through matrix converter

Figure 1 is a general block diagram of the DTC scheme. Stator flux $\hat{\psi}_s^*$ and torque T_e^* commands were compared with the estimator output. The results of these comparisons that is, flux and torque errors, were then sent to a separate hysteresis controller. Switching strategy is the most important part of the control scheme, as it affects directly, drive performance. Lee et al. (2007), Lee and Blaabjerg (2008) and Ortega et al. (2010) propose strategies that combine matrix-converter advantages with DTC-scheme benefits. Lee and Blaabjerg (2007) present comparisons between classical DTC that uses "matrix converter" and the proposed method. The 3 × 3 "matrix converter" in Figure 2a is of the highest practical interest as it connects a three-phase voltage source with a three-phase load (typically a motor). There are 27 possible switching configurations, but only 21 of them are useful in DTC algorithm (Casadei et al., 2001). Table 1 lists the 21 voltage vectors. Figure 2b shows the first 18 voltage vectors having fixed

Table 1. 3 × 3 matrix converter.

Switching combinations	On switches			Voltage vectors value		σValue	β value
				v_o	α_o		
+1	S_{Aa}	S_{Bb}	S_{Bc}	$2/3v_{AB}$	0	$2/\sqrt{3}V_m\cos(\omega t+\pi/6)$	0
-1	S_{Ba}	S_{Ab}	S_{Ac}	$-2/3v_{AB}$	0	$-2/\sqrt{3}V_m\cos(\omega t+\pi/6)$	0
+2	S_{Ba}	S_{Cb}	S_{Cc}	$2/3v_{BC}$	0	$2/\sqrt{3}V_m\cos(\omega t-\pi/2)$	0
-2	S_{Ca}	S_{Bb}	S_{Bc}	$-2/3v_{BC}$	0	$-2/\sqrt{3}V_m\cos(\omega t-\pi/2)$	0
+3	S_{Ca}	S_{Ab}	S_{Ac}	$2/3v_{CA}$	0	$2/\sqrt{3}V_m\cos(\omega t+5\pi/6)$	0
-3	S_{Aa}	S_{Cb}	S_{Cc}	$-2/3v_{CA}$	0	$-2/\sqrt{3}V_m\cos(\omega t+5\pi/6)$	0
+4	S_{Ba}	S_{Ab}	S_{Bc}	$2/3v_{AB}$	$2\pi/3$	$-1/\sqrt{3}V_m\cos(\omega t+\pi/6)$	$V_m\cos(\omega t+\pi/6)$
-4	S_{Aa}	S_{Bb}	S_{Ac}	$-2/3v_{AB}$	$2\pi/3$	$1/\sqrt{3}V_m\cos(\omega t+\pi/6)$	$-V_m\cos(\omega t+\pi/6)$
+5	S_{Ca}	S_{Bb}	S_{Cc}	$2/3v_{BC}$	$2\pi/3$	$-1/\sqrt{3}V_m\cos(\omega t-\pi/2)$	$V_m\cos(\omega t-\pi/2)$
-5	S_{Ba}	S_{Ca}	S_{Bc}	$-2/3v_{BC}$	$2\pi/3$	$1/\sqrt{3}V_m\cos(\omega t-\pi/2)$	$-V_m\cos(\omega t-\pi/2)$
+6	S_{Aa}	S_{Cb}	S_{Ac}	$2/3v_{CA}$	$2\pi/3$	$-1/\sqrt{3}V_m\cos(\omega t+5\pi/6)$	$V_m\cos(\omega t+5\pi/6)$
-6	S_{Ca}	S_{Ab}	S_{Cc}	$-2/3v_{CA}$	$2\pi/3$	$1/\sqrt{3}V_m\cos(\omega t+5\pi/6)$	$-V_m\cos(\omega t+5\pi/6)$
+7	S_{Ba}	S_{Bb}	S_{Ac}	$2/3v_{AB}$	$4\pi/3$	$-1/\sqrt{3}V_m\cos(\omega t+\pi/6)$	$-V_m\cos(\omega t+\pi/6)$
-7	S_{Aa}	S_{Ab}	S_{Bc}	$-2/3v_{AB}$	$4\pi/3$	$1/\sqrt{3}V_m\cos(\omega t+\pi/6)$	$V_m\cos(\omega t+\pi/6)$
+8	S_{Ca}	S_{Cb}	S_{Bc}	$2/3v_{BC}$	$4\pi/3$	$-1/\sqrt{3}V_m\cos(\omega t-\pi/2)$	$-V_m\cos(\omega t-\pi/2)$
-8	S_{Ba}	S_{Bb}	S_{Cc}	$-2/3v_{BC}$	$4\pi/3$	$1/\sqrt{3}V_m\cos(\omega t-\pi/2)$	$V_m\cos(\omega t-\pi/2)$
+9	S_{Aa}	S_{Ab}	S_{Cc}	$2/3v_{CA}$	$4\pi/3$	$-1/\sqrt{3}V_m\cos(\omega t+5\pi/6)$	$-V_m\cos(\omega t+5\pi/6)$
-9	S_{Ca}	S_{Cb}	S_{Ac}	$-2/3v_{CA}$	$4\pi/3$	$1/\sqrt{3}V_m\cos(\omega t+5\pi/6)$	$V_m\cos(\omega t+5\pi/6)$
0_A	S_{Aa}	S_{Ab}	S_{Ac}	0	…	0	0
0_B	S_{Ba}	S_{Bb}	S_{Bc}	0	…	0	0
0_C	S_{Ca}	S_{Cb}	S_{Cc}	0	…	0	0

directions; they correspond to active vectors, and their magnitude depends on input voltages (Table 1). The third and fourth columns of Table 1 introduce a stationary reference frame, α and β components of the "matrix converter's" output voltage vectors. The last three switching configurations determine zero-output voltage vectors (which shall be named zero vectors).

METHODOLOGY

Neglecting stator-resistance voltage drop, an induction machine's flux equation can be expressed as:

$$\overrightarrow{\Delta\psi_s}=\vec{V}_s\cdot\Delta t \quad (1)$$

Radial (V_{sr}) component of the stator-voltage space vector (V_s) changes the stator flux magnitude, and the tangential (V_{st}) component changes the stator flux angle (Figure 3). They can be expressed as:

$$V_{sr}=V_{s\alpha}\cos\theta+V_{s\beta}\sin\theta \quad (2)$$

$$V_{st}=-V_{s\alpha}\sin\theta+V_{s\beta}\cos\theta \quad (3)$$

Where θ is the angle of stator flux vector $\vec{\psi}_s$.

Figure 4 shows how the small magnitude of $\overrightarrow{\Delta\psi_s}$ is compared with $\vec{\psi}_s$ magnitude, the following equation could result:

$$\Delta|\vec{\psi}_s|=|\vec{\psi}_{s2}|-|\vec{\psi}_{s1}|\cong V_{sr}\cdot\Delta t \quad (4)$$

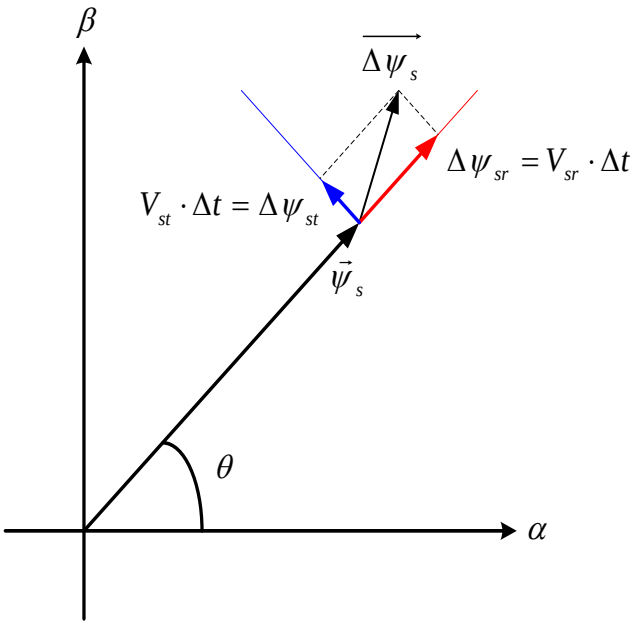

Figure 3. Radial and tangential components stator-flux vector.

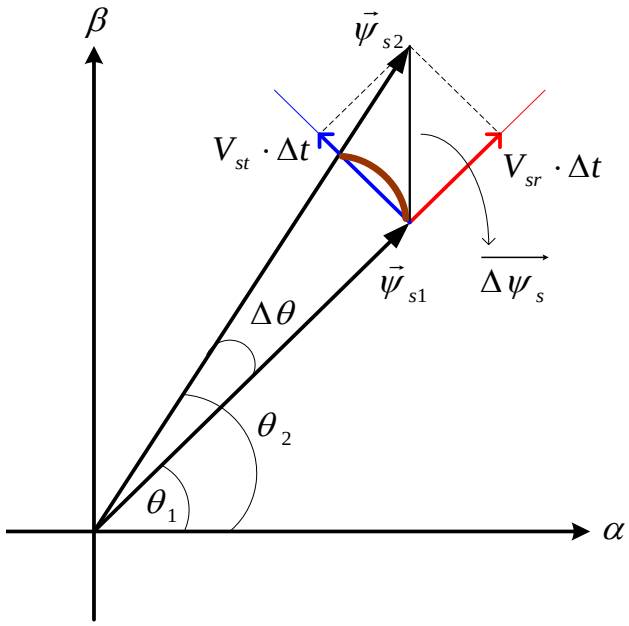

Figure 4. Amplitude and angle variation resulting from application of voltage vector by matrix converter.

Figure 4 shows $\Delta|\vec{\psi}_s|$ representing magnitude variation of stator-flux vector post-application of stator-voltage vector $\vec{V}_s$, for time increment Δt. Substituting V_{sr} from Equation (2) in (4) gives:

$$\Delta|\vec{\psi}_s| = \left(V_{s\alpha}\cos\theta_1 + V_{s\beta}\sin\theta_1\right)\cdot\Delta t \tag{5}$$

Which reveals the influencing characteristics of each voltage vector for magnitude variation of stator-flux vector.

Electromagnetic torque of induction machines can be expressed by:

$$T_e = \frac{3}{2}\cdot\frac{P}{2}\cdot\frac{L_m}{\sigma\cdot L_s\cdot L_r}\cdot|\vec{\psi}_r|\cdot|\vec{\psi}_s|\sin\gamma \tag{6}$$

Where γ and σ are load angle and leakage factor, respectively.

For an expression describing torque variation caused by applying voltage space vector $\vec{V}_s$ during Δt, equation (6) is differentiated, assuming constant magnitude for rotor flux vector during Δt owing to rotor's large time constant (Krause, 1986).

$$\Delta T_e = k_T\cdot|\vec{\psi}_r|\cdot\left(\frac{d|\vec{\psi}_s|}{dt}\cdot\sin\gamma + \frac{d(\sin\gamma)}{dt}\cdot|\vec{\psi}_s|\right)\Bigg|_{t_0}\cdot\Delta t \tag{7}$$

Where t_0 denotes the time, pre-application of voltage vector, and k_T a constant defined as:

$$k_T = \frac{3}{2}\cdot\frac{P}{2}\cdot\frac{L_m}{\sigma\cdot L_s\cdot L_r} \tag{8}$$

Rearranging Equation (7) gives:

$$\Delta T_e = k_T\cdot|\vec{\psi}_r|\cdot\left(\frac{d|\vec{\psi}_s|}{dt}\Bigg|_{t_0}\sin\gamma_1 + \frac{d\gamma}{dt}\Bigg|_{t_0}\cos\gamma_1\cdot|\vec{\psi}_{s1}|\right)\cdot\Delta t \tag{9}$$

Where index 1 is magnitude of the specified variables at exactly t_0 (time just before application of voltage vector).

Equation (5) leads to:

$$\frac{d|\vec{\psi}_s|}{dt}\Bigg|_{t_0} = V_{s\alpha}\cos\theta_1 + V_{s\beta}\sin\theta_1 \tag{10}$$

Where θ_1 is the angle of stator flux vector $\vec{\psi}_s$ pre- application of voltage vector $\vec{V}_s$.

Figure 5 shows flux-vector variations, pre, and post, voltage-vector applications by "matrix converter." Indices 1 and 2 respectively indicate the flux situations pre, and post, applications of voltage vector. For example, γ_1 is the angle between stator and rotor flux vectors pre-application of voltage vector. $\Delta\theta$ and $\Delta\zeta$ are respectively variations of stator, and of rotor, flux vector angles during Δt. Variation of load angle $\Delta\gamma$ during this time is calculated as:

$$\Delta\gamma = \Delta\theta - \Delta\zeta \tag{11}$$

Figure 4 shows application of voltage vector $\vec{V}_s$ increasing stator flux angle $\Delta\theta$ given by:

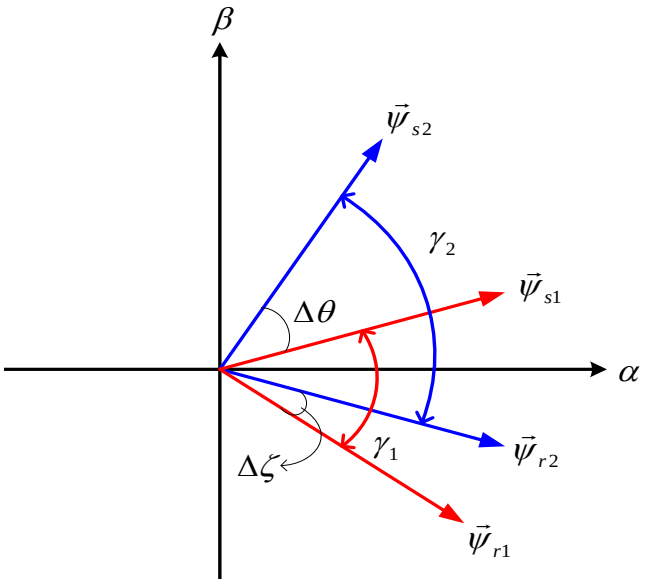

Figure 5. Variation of flux vectors pre and post applications of voltage vector.

$$\Delta\theta \cdot \left|\vec{\psi}_{s1}\right| \cong V_{st} \cdot \Delta t \tag{12}$$

Substituting V_{st} from Equation (3) in (12) yields:

$$\Delta\theta = \frac{-V_{s\alpha}\sin\theta_1 + V_{s\beta}\cos\theta_1}{\left|\vec{\psi}_{s1}\right|} \cdot \Delta t \tag{13}$$

Hence:

$$\left.\frac{d\theta}{dt}\right|_{t_0} = \frac{-V_{s\alpha}\sin\theta_1 + V_{s\beta}\cos\theta_1}{\left|\vec{\psi}_{s1}\right|} \tag{14}$$

Considering rotor-flux rotating with synchronous speed ω_s while magnitude remains nearly constant during Δt, the following equation can be explored for angle variation of rotor-flux vector:

$$\Delta\zeta = \omega_s \cdot \Delta t \quad \Rightarrow \quad \left.\frac{d\zeta}{dt}\right|_{t_0} = \omega_s \tag{15}$$

Equations 11, 14 and 15 can be written as:

$$\left.\frac{d\gamma}{dt}\right|_{t_0} = \left.\frac{d\theta}{dt}\right|_{t_0} - \left.\frac{d\zeta}{dt}\right|_{t_0} = \frac{-V_{s\alpha}\sin\theta_1 + V_{s\beta}\cos\theta_1}{\left|\vec{\psi}_{s1}\right|} - \omega_s \tag{16}$$

Substituting Equations (10) and (16) in (9), expression for the torque variation to be explored is:

$$\Delta T_e = k_T \cdot \left|\vec{\psi}_r\right| \cdot (x - y) \cdot \Delta t \tag{17}$$

Where x and y are:

$$\begin{aligned} x &= (V_{s\alpha}\cos\theta_1 + V_{s\beta}\sin\theta_1)\sin\gamma_1 \\ y &= (V_{s\alpha}\sin\theta_1 - V_{s\beta}\cos\theta_1 + \omega_s\left|\vec{\psi}_{s1}\right|)\cos\gamma_1 \end{aligned} \tag{18}$$

For normalization of Equations (5) and (17), rating values of the machine studied can be selected as base values:

$$V_m = \omega \cdot \psi_m \quad \Rightarrow \quad \psi_{base} = \frac{V_{base}}{\omega_{base}} = \frac{V_m}{\omega} \tag{19}$$

And,

$$T_{e,base} = \frac{3}{2} \cdot \frac{P}{2} \cdot \frac{L_m}{\sigma \cdot L_s \cdot L_r} \cdot \left|\vec{\psi}_{r,base}\right| \cdot \left|\vec{\psi}_{s,base}\right| \cdot \sin\gamma_{base} \tag{20}$$

Where γ_{base} is the load angle at rated condition. We can write:

$$\Delta\left|\vec{\psi}_s\right|_{pu} = \frac{\Delta\left|\vec{\psi}_s\right|}{\psi_{base}} = \frac{(V_{s\alpha}\cos\theta_1 + V_{s\beta}\sin\theta_1) \cdot \Delta t}{V_{base}/\omega_{base}} \tag{21}$$

Per-unit equation for flux variation results:

$$\Delta\left|\vec{\psi}_s\right|_{pu} = (V_{s\alpha,pu}\cos\theta_1 + V_{s\beta,pu}\sin\theta_1) \cdot k_1 \tag{22}$$

Where $k_1 = \omega_{base} \cdot \Delta t$.

As earlier mentioned, to express torque variation in per-unit equation, Equation (6) is used in the following format:

$$\Delta T_{e,pu} = \frac{\Delta T_e}{T_{e,base}} = \frac{k_T \cdot \left|\vec{\psi}_r\right| \cdot (x - y) \cdot \Delta t}{k_T \cdot \left|\vec{\psi}_{r,base}\right| \cdot \left|\vec{\psi}_{s,base}\right| \sin\gamma_{base}} \tag{23}$$

Simplifying Equation (23) yields:

$$\Delta T_{e,pu} = \left|\vec{\psi}_{r,pu}\right| \cdot (x_{pu} - y_{pu}) \cdot \Delta t \tag{24}$$

Where:

$$\begin{aligned} x_{pu} &= (V_{s\alpha,pu}\cos\theta_1 + V_{s\beta,pu}\sin\theta_1) \cdot \frac{\sin\gamma_1}{\sin\gamma_{base}} \cdot \omega_{base} \\ y_{pu} &= \left((V_{s\alpha,pu}\sin\theta_1 - V_{s\beta,pu}\cos\theta_1) \cdot \omega_{base} + \omega_s \cdot \left|\vec{\psi}_{s1}\right|_{pu}\right) \cdot \frac{\cos\gamma_1}{\sin\gamma_{base}} \end{aligned} \tag{25}$$

Equation 24 for torque variation per-unit can be rewritten as:

$$\begin{aligned} \Delta T_{e,pu} = \left|\vec{\psi}_{r,pu}\right| \cdot \Big\{ & \Delta\left|\vec{\psi}_s\right|_{pu} (\sin\gamma_1)_{pu} - \\ & \left((V_{s\alpha,pu}\sin\theta_1 - V_{s\beta,pu}\cos\theta_1) + \right. \\ & \left. (2/p) \cdot \omega_{s,pu} \cdot \left|\vec{\psi}_{s1}\right|_{pu}\right) \cdot \sqrt{k_2 - (\sin\gamma_1)_{pu}^{\,2}} \cdot k_1 \Big\} \end{aligned} \tag{26}$$

Where $k_2 = \dfrac{1}{(\sin\gamma_{base})^2}$.

Expression of Equation (26) seems applicable to any induction motor drive of any rating, but because of its dependence on γ_{base},

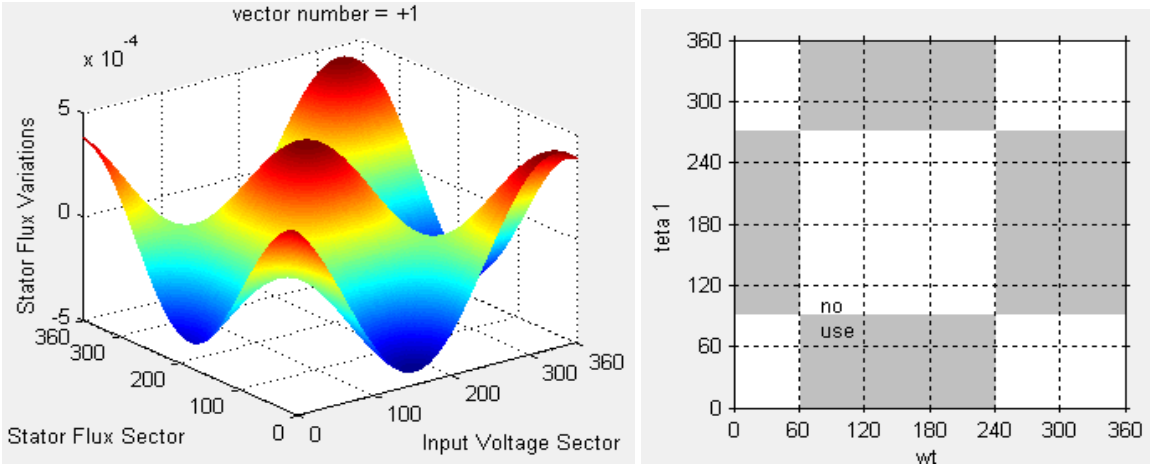

Figure 6. Stator flux vector variations in nominal work conditions of motor, in 60° sectors for V_{+1}. (a) stator-flux variation and (b) variation of flux-vector angle.

influencing characteristics of voltage vectors can differ in low power and high power applications.

RESULTS ANALYSIS

Voltage-vector effect on flux

For flux variations to different voltage vectors, α and β components of each vector were substituted based on per-unit, and equations obtained, for example, evaluating flux variation with α and β components of V_{+1} converted into per-unit based on machine's rated voltage (V_m) yields Equation (5):

$$\begin{cases} v_{+1\alpha,pu} = \dfrac{v_{+1\alpha}}{V_m} = \dfrac{2}{\sqrt{3}} \cos(\omega t + \dfrac{\pi}{6}) \\ v_{+1\beta,pu} = 0 \end{cases} \quad (27)$$

Substituting α and β components related to V_{+1} in flux-variation equation gives Equation (6):

$$\Delta|\vec{\psi}_s|_{pu,+1} = \frac{2}{\sqrt{3}} \cdot (\cos(\omega t + \pi/6) \times \cos\theta_1) \cdot (120\pi) \times 10^{-6} \quad (28)$$

Referring to Equation 6, rated frequency of motor was 60 Hz, and sampling time-interval considered was 1 µs. Two figures compare voltage-vector effect on flux; Figure 6a is stator-flux variation in terms of ωt and θ_1,, and Figure 6b is θ_1 versus ωt, referring to the positive (white) ($\Delta|\vec{\psi}_s|_{pu} \geq 0$) and the negative (gray) ($\Delta|\vec{\psi}_s|_{pu} < 0$) regions of the flux variations in Figure 6a. Note that in some regions, use of voltage vector when space vector is divided into six 60° sectors is impossible. Figure 6b shows one of the regions (ωt<120 and θ >60); flux in one half of it is positive (V_{+1} increases the stator flux) and in the other half it is negative (V_{+1} decreases the stator flux). Use of V_{+1} in this region is thus not allowed. The degrees of freedom rose with division of the space vector into twelve 30° sectors, in which condition voltage vector V_{+1} could be used in both regions, behaving two ways: flux increasing and flux decreasing). Figure 7 confirmed the assertion (with V_{-1} and V_{+1} sketched), showing no useless areas existing in which vectors V_{-1} and V_{+1} could not be used if the space vector was divided into 30° sectors, that is, behavior characteristic of each vector's stator-flux variation did not change in any of the areas. Thus designing of a switching table for 30° sectors (sectors of stator flux vectors (θ_1) and sectors of input voltage (ωt)) is appropriate to increase degrees of freedom.

As Figure 7 shows, behavior of flux variation for vector voltage V_{+1} is opposite to voltage vector V_{-1}, that is, in each sector, flux variation for voltage vector V_{+1} is positive, but negative for vector voltage V_{-1}. This statement is true for all vectors (for example, V_{+5} and V_{-5}, etc.).

Voltage-vector effect on torque

Table 2 lists 3-phase induction motor parameters, with 2250 hp, 60Hz, and 4-pole selected for test-motor simulation (Krause, 1986). Machine structure and specifications such as number of poles and load angle

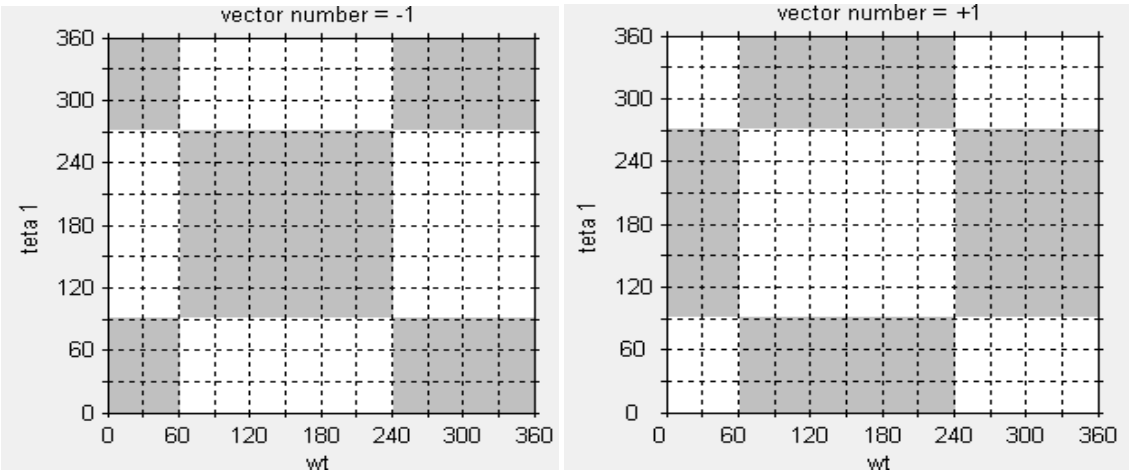

Figure 7. Stator-flux behavioral characteristic for V_{+1} and V_{-1}, in 30° sectors.

Table 2. Specifications and parameters of the 3-phase test induction-motor

volts	*rpm*	J kg/m^2	R'_r *ohms*	X'_{lr} *ohms*	X_M *ohms*	X_{ls} *ohms*	R_s *ohms*	I_{base} *amps*	$T_{e,base}$ $N.m$
2300	1786	63/87	0/022	0/226	13/04	0/226	0/029	420	8900

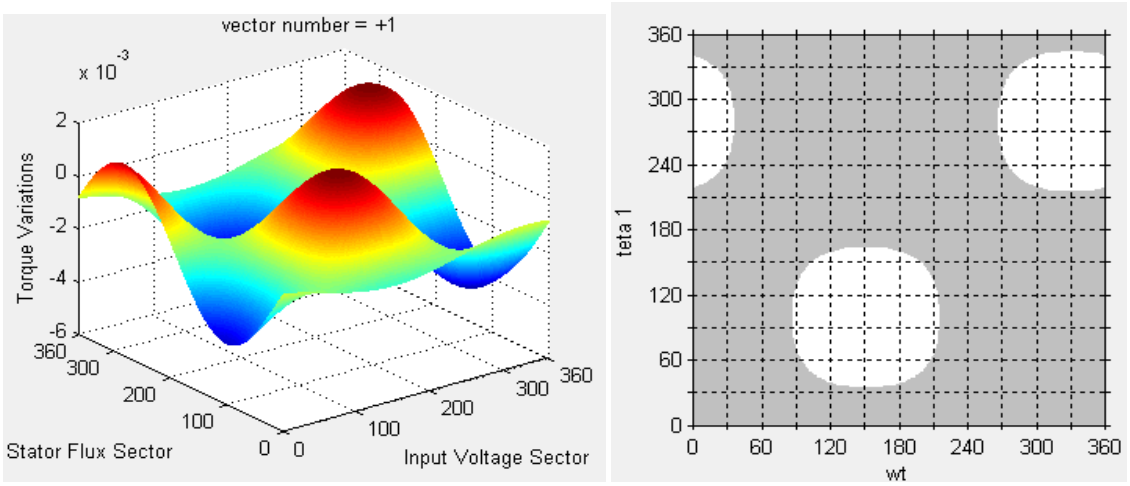

(a) (b)

Figure 8. Torque variation in nominal motor work conditions in 30° sectors for V_{+1}. (a) torque variation and (b) torque-angle variation.

(γ_{base}) affect the rate of machine-torque variation. This work designed the proper switching table according to the motor parameters suggested, which were considered for extraction of the proper vectors. Choice of parameters did not affect the method proposed here, as the method is comprehensive and good for control of any motor. Figure 8a shows torque variation in terms of ωt and θ_1, and Figure 8b is θ_1 versus ωt. The torque variation was plotted

Table 3. Results for effect of V_{+1} vector on torque variation (NU = no use)

L	1	2	3	4	5	6	7	8	9	10	11	12
$k=1$	-	-	-	-	-	-	-	-	-	-	-	-
$k=2$	-	-	-	nu	nu	nu	nu	-	-	-	-	-

for nominal work conditions of the motor, in 30° sectors, for V_{-1}. By replacing per-unit values of α and ß components related to V_{+1}, a torque-variation curve due to applied voltage vector in motor rated conditions could be drawn (*T1* = 1 *pu*, ω_m= 1 *pu*). As before, two figures were extracted for torque variation (ΔT_e, *pu*). Table 3 lists the proper regions in which V_{+1} had been proven to have sustainable impression characteristics L and K respectively indicating the number of voltage-input sectors and the number of flux-vector sectors. For example, L = 1 means $0 \le \omega t \le 30^0$, and L = 2 means $30^\circ \le \omega t \le 60^0$, and also in stator-flux vector sector, k = 1 means $0 \le \theta_1 \le 30^0$, and k = 2 means $30^\circ \le \theta_1 \le 60^0$. Table 3 shows negative (-) sign, the reduced torque and NU (no use) marks changed-state areas; torque did not increase in any of the regions. Similar situations were considered for the rest of the sectors. Only the resultants of the first and the second sectors of the stator-flux vector, however, were mentioned in the table.

Vector suitable for control

To examine the effect of 18 active voltage vectors produced by "matrix converter" have on flux and torque, a procedure similar to that applied for V_{+1} was applied. Vectors with fixed-effect characteristic in the 30° sectors were then chosen as suitable for control (increase/decrease stator flux and motor torque). Table 4 lists the results, where H_φ and H_{Te} show flux and torque hysteresis output controller. Table 4 was produced for the stator flux in the first and the second sectors, but owing to symmetry conditions in space vector results were valid also for the remaining sectors. Note that, H_ω = +1 and H_ω = -1 were respectively increase-flux and decrease-flux commands, in which order *the* = +1 and H_{Te} = -1 introduced increase-torque and decrease-torque commands. Table 4 lists the results for the first 6 sectors of the input voltage. The results for the 6 remaining sectors contrast those of the first 6 sectors, for example, vectors +9 and -9 are respectively flux increase and torque increase, in the first sector (*L* = 1) and the 7th sector (*L* = 7), respectively, of the input voltage. Another example is in the second sector (*L* = 2) of the input voltage, where vector -6 is both reduced flux and also increased torque; vector +6 decreased flux and increased torque in the 8th sector (*L* = 8) of the input voltage.

Conclusions

It presents the selection of the voltage vectors appropriate for control of flux and torque in machine nominal work conditions. Machine speed and load angle, both proportional to torque, affect torque variation through voltage vector applied by "matrix converter". Each voltage-vector's effect in various speed ranges and loads thus should be investigated. Table 4 shows that in some sectors, many vectors have the same effect. It indicates the degrees of freedom in selecting voltage vector, for application of "matrix converter" to DTC. The degrees of freedom were used to improve DTC operation in terms of current ripple, torque, switching frequency and control of input power factor. Note that in some sectors, there were no selectable regions - one of "matrix converter's" limitations.

Nomenclature

***α*,** component of the matrix converter; ***β*,** component of the matrix converter; $\hat{\psi}_S^*$, Stator flux command; T_e^*, torque command; $\overrightarrow{\Delta\psi_S}$, stator flux vector variation; V_{sr}, radial component of voltage space vector; V_{st}, tangential component of voltage space vector; $\vec{\psi}_S$, stator flux vector; ***θ*,** angle of stator flux vector; T_e, electromagnetic torque of induction machines; ***γ*,** load angle; ***σ*,** leakage factor; k_T, constant value; t_0, Initial time; γ_1, angle between stator and rotor flux vectors; $\Delta\theta$, variations of stator flux vector angles; $\Delta\zeta$, variations of rotor flux vector angles; $\Delta\gamma$, variation of load angle; $\vec{V}_S$, voltage vector; θ_1, the angle of stator flux vector; Δt, time interval; ω_s, synchronous speed; ΔT_e, variation of electromagnetic torque; ***x*,** horizontal direction in cartesian coordination; ***y*,** vertical direction in cartesian coordination; γ_{base}, load angle at rated condition; $\Delta|\vec{\psi}_S|_{pu}$, stator flux variation on per unit; $\Delta T_{e,\,pu}$, torque variation on per unit; k_1, flux variation coefficient; k_2, torque variation coefficient; V_m, rated voltage; V_{+1}, voltage vector first order in positive region; V_{-1}, voltage vector first order in negative region; H_φ, flux hysteresis output controller; H_{Te}, torque hysteresis output controller; ***L*,** number of sector; L_m, mutual leakage inductance; L_s,

Table 4. Degrees of freedom in selecting appropriate values for the first and the second stator flux vectors.

Proper vectors $0 \leq \theta_1 \leq 30°$ (k = 1)				
H_φ	+1		-1	
H_{Te}	+1	-1	+1	-1
L = 1	+9	+1, +2, +6 -3, -4, -5	-6	+3, +7, +8 -1, -2, -9
L = 2	+9	+1, +2, +6 -3, -4, -5	-6	+3, +7, +8 -1, -2, -9
L = 3	-8	+2, +4, +6 -1, -3, -5	+5	+1, +3, +8 -2, -7, -9
L = 4	-8	+2, +4, +6 -1, -3, -5	+5	+1, +3, +8 -2, -7, -9
L = 5	+7	+2, +3, +4 -1, -5, -6	-4	+1, +8, +9 -2, -3, -7
L = 6	+7	+2, +3, +4 -1, -5, -6	-4	+1, +8, +9 -2, -3, -7
Proper vectors $30° \leq \theta_1 \leq 60°$ (k = 2)				
H_φ	+1		-1	
H_{Te}	+1	-1	+1	-1
L = 1	+4 -6	+1, +2 -3, -8	-	+6, +7, +8 -2, -4, -5, -9
L = 2	+5 -6	+1, +2 -3, -7	-	+6, +7, +8 -1, -4, -5, -9
L = 3	+5 -6	+2, +7 -1, -3	-	+1, +4, +6, +8 -5, -7, -9
L = 4	+5 -4	+2, +9 -1, -3	-	+3, +4, +6, +8 -5, -7, -9
L = 5	+5 -4	+2, +3 -1, -9	-	+4, +8, +9 -3, -5, -6, -7
L = 6	+6 -4	+2, +3 -1, -8	-	+4, +8, +9 -2, -5, -6, -7

stator leakage inductance; $V_{s\alpha}$, α component of stator voltage.

REFERENCES

Bose BK (2002). Modern Power Electronics and AC Drives. Prentice-Hall PTR.

Casadei D, Serra G, Tani A (2001). The Use of Matrix Converter in Direct Torque Control of Induction Machines. IEEE Trans. Ind. Electron., 48(6): 1057-1064.

Hojabri H, Mokhtari H, Chang L (2011). a Generalized Technique of Modeling, Analysis, and Control of a Matrix Converter Using SVD. IEEE Trans. Ind. Electron., 58(3): 949-959.

Klumpner C, Blaabjerg F, Boldea I, Nielsen P (2006). New Modulation Method for Matrix Converters. IEEE Trans. Ind. Appl., 42(3): 797-806.

Krause PC (1986). Analysis of Electric Machinery. McGraw-Hill.

Lascu C, Boldea I, Blaabjerg F (2000). A Modified Direct Torque Control for Induction Motor Sensorless Drive. IEEE Trans. Ind. Appl., 36(1): 122-130.

Lee K, Blaabjerg F (2008). Sensorless DTC-SVM for Induction Motor Driven by a Matrix Converter Using a Parameter Estimation Strategy, IEEE Trans. Ind. Electron., 55(2): 512-521.

Lee K, Blaabjerg F (2007). An Improved DTC-SVM Method for Sensorless Matrix Converter Drives Using an Overmodulation Strategy and a Simple Nonlinearity Compensation. IEEE Trans. Ind. Electron., 54(6): 3155-3166.

Lee K, Blaabjerg F, Yoon TW (2007). Speed-Sensorless DTC-SVM for Matrix Converter Drives with Simple Nonlinearity Compensation. IEEE Trans. Ind. Appl., 43(6): 1639-1649.

Ortega C, Arias A, Caruana C, Balcells J, Asher GM (2010). Improved Waveform Quality in the Direct Torque Control of Matrix-Converter-Fed PMSM Drives. IEEE Trans. Ind. Electron., 57(6): 2101-2110.

Takahashi I, Noguchi T (1986). A new quick response and high-efficiency control strategy of an induction motor. IEEE Trans. Ind. Appl., IA-22(5): 820-827.

Vargas R, Ammann U, Hudoffsky B, Rodriguez J, Wheeler P (2010). Predictive Torque Control of an Induction Machine Fed by a Matrix Converter with Reactive Input Power Control. IEEE Trans. Power Electron., 25(6): 1426-1438.

Zaid SA, Mahgoub OA, El-Metwally KA (2010). Implementation of a new fast Direct Torque Control algorithm for induction motor drives. Electric Power Appl., IET.J. Electric Power Appl., 4(5).